Knowl. Manag. Aquat. Ecosyst. 2022, 423, 23
© N.Y. Flores *et al.*, Published by EDP Sciences 2022
https://doi.org/10.1051/kmae/2022019

www.kmae-journal.org

Knowledge & Management of Aquatic Ecosystems

Journal fully supported by Office français de la biodiversité

RESEARCH PAPER OPEN ACCESS

3D upstream passability of novel river training structures by migratory fish in the river Waal

Natasha Y. Flores*, Frank P.L. Collas and Rob S.E.W. Leuven

Department of Animal Ecology and Physiology, Radboud Institute for Biology and Environmental Sciences (RIBES), Radboud University, P.O. Box 9010, 6500 GL Nijmegen, the Netherlands

Received: 8 October 2021 / Accepted: 8 July 2022

Abstract – Longitudinal training dams (LTDs) are novel river training structures that divide a river into a main navigation channel and protected shore channels. High velocities at the inflows of shore channels constructed in the river Waal (The Netherlands) pose a potential bottleneck for migratory fish species swimming upstream. This study assessed the passability of the inflows using flow velocity datasets from governmental monitoring campaigns collected with an ADCP during high river discharges (Q = 3489–5066 m^3/s at Lobith monitoring station). The swimming performance of several migratory fish species were estimated from their total lengths (TLs). A new 3D approach to visualize the flow velocity data using Voxler® software is presented. *Gasterosteus aculeatus aculeatus* was the only fish species with an adult life stage unable to pass the 9 cases tested due to its small size. The juvenile European eel and thicklip grey mullet passed 1 and 0 of the cases, respectively. The most upstream inflow, located in the inner bend of the river, was the most passable. We recommend maximizing the cross-sectional area of the inflow sills in order to reduce the flow velocities experienced by migrating fish during high river discharges. This approach may be useful to assess passability at other locations and training structures.

Keywords: ADCP measurements / diadromous fish / longitudinal training dam / swimming performance / shore channel

1 Introduction

Migratory fish species are among the most threatened fish species in Europe with a population decline of 93% in 2020 (Deinet *et al.*, 2020). These fish species have been greatly impacted by climate change, overfishing, inland navigation, habitat loss and fragmentation among other anthropogenic pressures (Wolter and Arlinghaus, 2003, 2004; Kucera-Hirzinger *et al.*, 2009; Limburg and Waldman, 2009; Zajicek *et al.*, 2018; Grill *et al.*, 2019). Climate change is expected to result in higher temperatures and more frequent and longer peak river discharges in Europe (Milly *et al.*, 2002; Van Vliet *et al.*, 2013), which could limit upstream migration of fish species due to high energy demands (Rand *et al.*, 2006). Migratory fish have complex life cycles that may involve migration from the sea to freshwater ecosystems (anadromous), from freshwater ecosystems to the sea (catadromous), or migration within freshwater ecosystems for spawning (potamodromous; Myers, 1949; Aarts and Nienhuis, 2003; Limburg and Waldman, 2009). The highly navigated river Rhine serves as habitat for several endangered and economically important diadromous fish species that migrate between the sea and freshwater, such as the European eel (*Anguilla anguilla*; Linnaeus, 1758), Atlantic salmon (*Salmo salar;* Linnaeus, 1758) and the extinct but reintroduced European sturgeon (*Acipenser sturio*; Linnaeus, 1758; Aarts and Nienhuis, 2003; Kottelat and Freyhof, 2007).

The river Waal is the major distributary of the river Rhine in the Netherlands taking on 65% of its total discharge (Raat, 2001). It is a heavily modified river with extensive hydraulic engineering structures, such as sluices and groynes, constructed in order to maintain water depths necessary for navigation (Uehlinger *et al.*, 2009). A possible new obstacle for upstream migrating fish in the river Waal are the three longitudinal training dams (LTDs) constructed in 2015. These LTDs are river training structures 3–4 km long parallel to the river's shoreline that divide the river into a main channel (230 m wide) and shore channels (80 m) protected from the effects of navigation on river banks and biodiversity (Eerden, 2013; Collas *et al.*, 2018). One of the LTD shore channels was estimated to carry 18–27% of the total river discharge (De Ruijsscher *et al.*, 2020). These structures were constructed with boulders, have an inflow with adjustable boulder sills that are generally fully submerged and an outflow into the main

*Corresponding author: n.flores@science.ru.nl

channel of the river. The LTDs are expected to be multifunctional aiding in the discharge of ice, providing flood safety, lowering maintenance costs, allowing for the development of novel habitats and maintaining adequate water levels for navigation in the main channel (Eerden, 2013; Collas *et al.*, 2018; De Ruijsscher *et al.*, 2018, 2020). The main channel of the river Waal is intensively navigated, this poses known risks for migrating fish species, such as wave action and increases in shear stress (Wolter and Arlinghaus, 2003; Zajicek *et al.*, 2018). The LTD shore channels might serve as migratory routes and refugia, but for that these sites must be passable. In a recent study on the habitat suitability of mussels, the inflows of the LTD shore channels had some of the highest estimated near-bottom flow velocity values in the shore channels (Flores *et al.*, 2022), areas near the riverbed tend to have lower flow velocities than the rest of the water column (Westenbroek, 2006), hence the inflows could pose a significant bottleneck for upstream migrating fish species. Additionally, high velocities at the inflows have also been observed in the field as the water funnels from the main channel into the shore channel creating areas of turbulence. Upstream passability of this possible bottleneck depends on the swimming performance of migratory fish species.

The swimming performance of fish has been classified into several swimming speeds. First, the sustained swimming speed which may be maintained for more than 200 min (Beamish, 1978). The prolonged swimming speed maintained for more than 20 s, but less than 200 min (Beamish, 1978). A subclass of the prolonged swimming speed is the critical swimming speed (U_{crit}) which may be maintained for up to 60 min (Brett, 1964). Finally, the burst swimming speed (U_{burst}) of a fish species is its highest speed and may be maintained for less than 20 s (Beamish, 1978).

The Directorate-General for Public Works and Water Management in the Netherlands (in Dutch: Rijkswaterstaat; RWS) has been monitoring the flow velocities of the three LTD inflows using an acoustic Doppler current profiler (ADCP) since their construction. This monitoring data has been collected with irregular frequency. From a precautionary principle, in this study we used the ADCP flow velocity monitoring datasets corresponding to the highest river discharges and estimated swimming performances for native migratory fish species to evaluate the passability of the LTD inflows for the years 2017–2019. Moreover, we present a 3-dimensional hydrostatic approach for evaluating the volume of the water column suitable for the upstream migration of fish using Voxler® (Golden Software, LLC). With this approach, we aim to answer the following research questions: (1) do ambient flow velocities in the inflows of the shore channels along LTDs in the river Waal provide migration pathways below the critical swimming speed of migratory fish species? (2) Do ambient flow velocities in the inflows of these channels provide migration pathways below the burst swimming speed of the fish species assessed?

2 Materials and methods

2.1 Migratory fish species and passability indicators

The current migratory pelagic and demersal fish species occurring in the river Waal were retrieved from Aarts and Nienhuis (2003), Kottelat and Freyhof (2007), Del Signore *et al.* (2016), Collas *et al.* (2018) and www.ravon.nl ($n = 14$). The total length (TL) for adult males was the most readily available length in www.fishbase.org for anadromous and potamodromous species. For catadromous fish species, the lengths for juveniles were obtained from Kottelat and Freyhof (2007). Standard lengths (SL) were converted to TL by using the species-specific equations from Binohlan *et al.* (2011). When field data was available the largest lengths were preferred. For instance, for sea trout and three-spined stickleback record lengths were used from www.beet.nl/records. The largest lengths available from field data were also used for the Allis shad (Collas *et al.*, 2021) and the Atlantic salmon (Hop and Van de Ven, 2021; see Supplementary Material Tab. S1).

Swimming performance data in the scientific literature differed in the experimental setup including water temperature, fish body lengths, life stages and time intervals among other variables. Hence we standardized the calculation of the swimming performances of the fish species by using equations available in the scientific literature. The passability indicators were obtained using linear regression equations relating the TL of fish species to U_{crit} and U_{burst} from Wolter and Arlinghaus (2003; 2004). These studies were completed using experimental data for fish species of different body types (*i.e.* eel, lamprey, salmon, *etc.*). The swimming speeds were calculated separately for small (up to 60 or 200 mm) and large (up to 1 m) fish by using size-specific equations (Wolter and Arlinghaus, 2003; 2004).

2.2 Flow velocity 3D lattices

The three LTD shore channels inflows were referred to in this study by the names of nearby towns; from upstream to downstream as Wamel (N51.887897, E5.485245), Dreumel (N51.881275, E5.442452) and Ophemert (N51.856219, E5.414687). Monitoring data from RWS surveys of the three LTD inflows (Fig. 1) collected with an ADCP operating at a frequency of 600 kHz were obtained in ACSII format for the years 2017, 2018 and 2019. To simplify the modeling using the novel 3D technique, areas for the models were selected based on dense coverage among the yearly datasets, spatial overlap, and field observations of turbulent flow within the shore channels. Based on the direct relationship between river discharge (Q), cross-sectional area (A) and flow velocity (V; $Q = A \times V$; Buchanan and Somers, 1969), it was assumed that high discharges would also result in the highest flow velocities at the study sites. Thus the passability assessment was limited to the available flow velocity datasets corresponding to the highest mean daily river discharges ($Q \geq 3489$ m^3/s) for each year at the Lobith monitoring station (www.waterinfo.rws.nl; Tab. 1). A total of 9 flow velocity datasets were assessed, one for each inflow per year.

The flow velocity datasets were filtered for dummy numbers and incomplete entries. The datasets were projected to the Amersfoort/RD_NEW coordinate system. Using ERSI ArcMAP 10.3.1, polygons of the inflows were manually digitized and used to extract the points within the inflows with the 'erase points' tool. The datasets were imported into Voxler® 4 software and the flow velocity magnitudes were

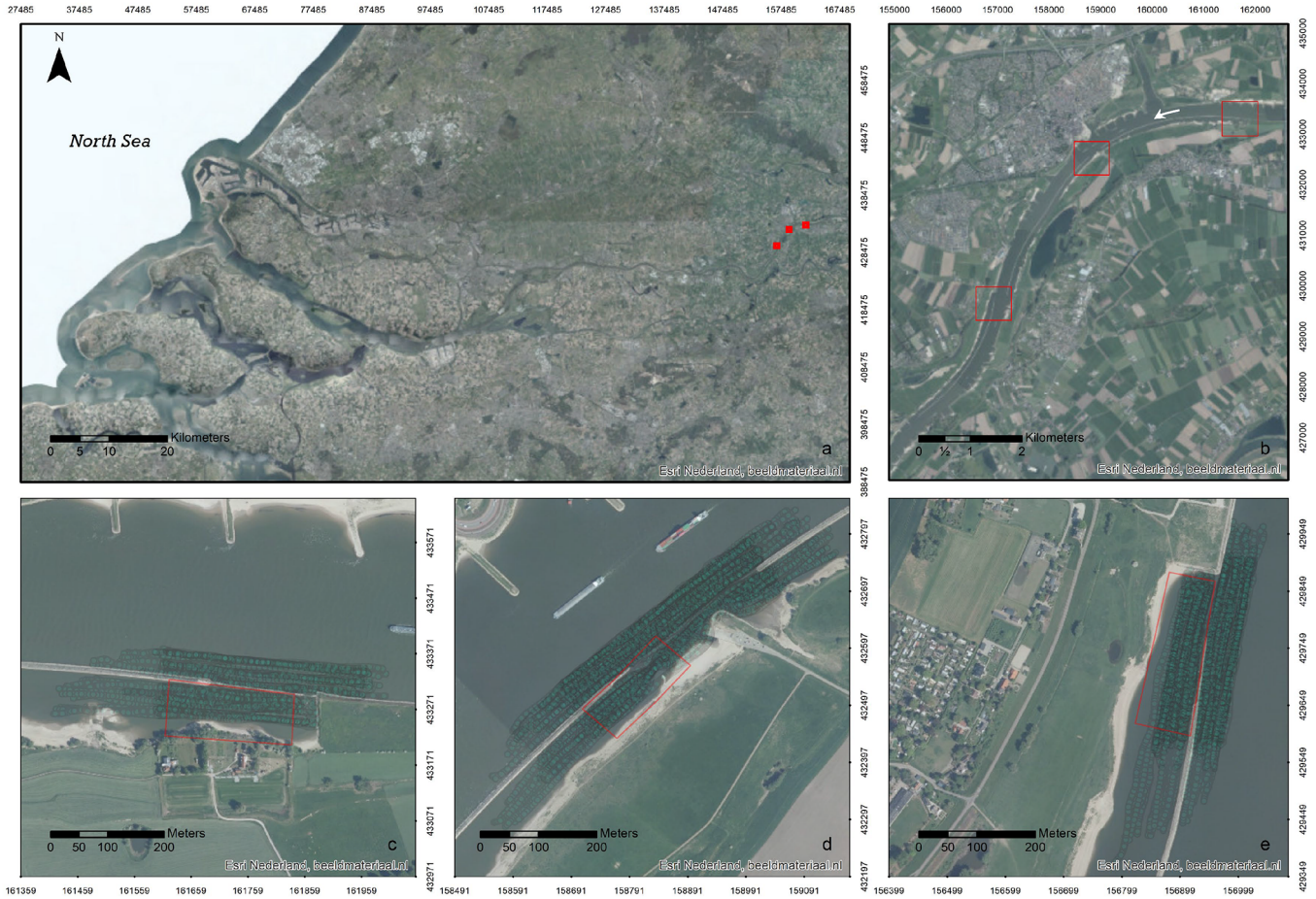

Fig. 1. (a) The delta of the river Rhine in the Netherlands with the location of the three LTD shore channel inflows in the river Waal marked by red squares, (b) an overview of the location of the three LTD inflows with a white arrow showing the main flow direction, (c) the inflow of the Wamel shore channel, (d) inflow of the Dreumel shore channel and (e) inflow of the Ophemert shore channel. The dark green points are the ADCP data collected during high river discharges between 2017 and 2019. The areas selected for the passability assessment are bounded by red squares. Aerial photographs source: Environmental Systems Research Institute (ESRI) Nederland, beeldmateriaal.nl.

gridded into 3D lattices using the inverse distance isotropic method (power = 30) and a resolution of 200 nodes per axis (total nodes = 8,000,000). The 'volrender' module was used to visualize the lattices and to improve the visualization of the datasets the lattices were transformed to 10 times the z-axis. Bottom height data included in the ADCP datasets was interpolated using kriging fitted to a spherical model (search radius $>$ 100 m) in Surfer software (Golden Software LLC) and imported into Voxler®. The z-axis was limited to the bottom height using the 'math' module to make all of the values at and below the riverbed equal to a dummy number out of the range of the flow velocities (*i.e.* if $z \leq B$, dummy number, A, where A is the flow velocity lattice and B is the interpolated bottom height). The 'isosurface' module was used to calculate the total volume of each lattice using the minimum flow velocity of the lattices prior to the riverbed removal as cut-offs to exclude the volumes below the riverbed.

2.3 LTD shore channel inflow passability by migratory fish

Assuming that the flow velocity direction was always the main flow direction, or downstream, the swimming performance of the migratory fish species were applied to the flow velocity lattices using the "math" module. Then the swimming speeds (U_{crit} or U_{burst}) of each fish species and the flow velocity lattices were subtracted resulting in new lattices showing the final swimming speed of the species (*i.e.* $U_{fish} = U_{crit} - V_{water}$; Katopodis, 1992). Minimum final upstream swimming speeds were calculated by subtracting the maximum of the flow velocity lattices from the swimming speeds to exclude the dummy number. The volumes of the lattice where forward motion was expected were calculated using the 'isosurface' module. This module outputs a volume based on an inputted threshold value ($\geq$ 0.05 m/s was used as threshold to exclude ~0 values). Comparison of this threshold value to other

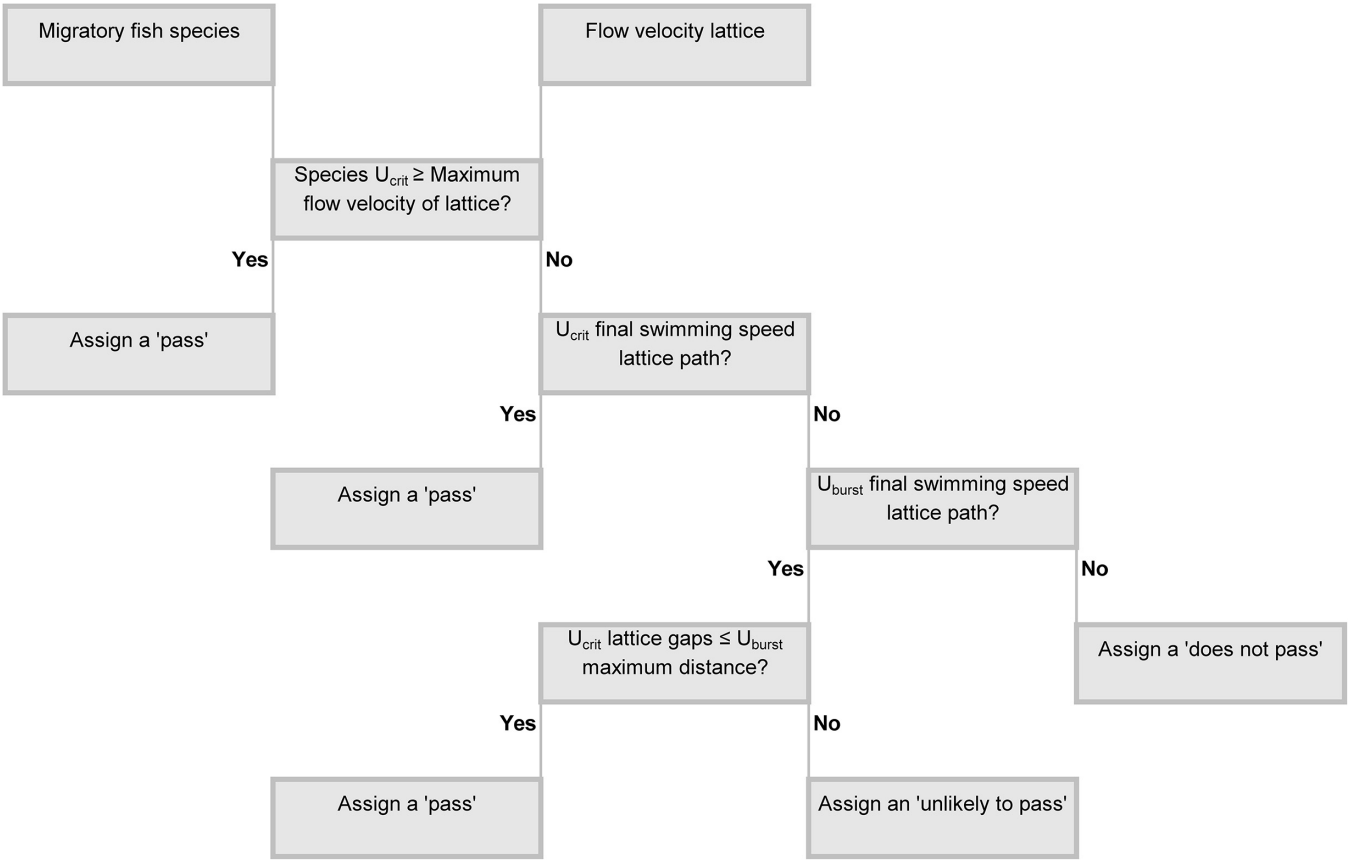

Fig. 2. Decision tree for the passability assessment of migratory fish species in the LTD shore channel inflows.

statistical significance levels, such as 0.001, yielded large (5–31%) volume differences for most cases tested when compared to a base threshold equal to 0.00001 (see Supplementary Material Tab. S2). Additionally, the U_{burst} and U_{crit} of freshwater fish juveniles were reported by Wolter and Arlinghaus (2004) to start at 0.05 and 0.06 m/s, respectively. Thus we considered final swimming speeds more than or equal (≥) to 0.05 m/s as an acceptable indicator for forward motion.

Passability was determined for each fish species based on the following conditions (Fig. 2):

- If the U_{crit} was more than or equal (≥) to the maximum flow velocity of the lattice a 'pass' was assigned for 100% of the lattice volume. For all other cases, the U_{crit} final swimming speed lattices were visually assessed for a continuous longitudinal path crossing from downstream to upstream. If a continuous path was observed a 'pass' was assigned.
- If a species did not pass using U_{crit}, then the U_{burst} final swimming speed lattices were assessed. The U_{burst} maximum distance was calculated assuming a burst performance time equal to 19.99 s. The U_{crit} and U_{burst} final swimming speed lattices were overlaid and their x and y-axes were used to assess distances. If there was a path in the U_{burst} final swimming speed lattices and the gaps left to pass in the U_{crit} final swimming speed lattices appeared less than or equal (≤) to the U_{burst} maximum distance, then a 'pass' was assigned. If the gaps appeared larger than this distance an 'unlikely to pass' was assigned. If no path was seen a 'does not pass' was assigned.

2.4 Statistical analysis

The count data for the total number of passes assigned for each inflow per year was checked for normality using a Shapiro test (R Core Team, 2021). For non-normally distributed data, any significant associations between the inflows, the year of data collection and the total number passes assigned were analyzed using a Chi-square test (R Core Team, 2021).

3 Results

3.1 Migratory fish species and passability indicators

The fish species selected for this study included two catadromous species that were assessed in their juvenile stage and had TLs equal to 32 and 70 mm for the thicklip grey mullet (*Chelon labrosus*; Risso, 1827) and the European eel, respectively. The TL for the adult fish ranged from 70 mm for the three-spined stickleback to 1250 mm for the European sturgeon. Calculated U_{crit} ranged from 0.25 m/s for the thicklip grey mullet to 3.99 m/s for the European sturgeon. Calculated U_{burst} ranged from 0.50 for the thicklip grey mullet to 7.83 m/s for the European sturgeon. Calculated U_{burst} maximum

Table 1. Summary information and descriptive statistics of the ADCP flow velocity datasets, 3D lattices and the passability results given as the percentage of the volume of the water column available for passage.

Parameter		*2017*			*2018*			*2019*		
		Wamel	**Dreumel**	**Ophemert**	**Wamel**	**Dreumel**	**Ophemert**	**Wamel**	**Dreumel**	**Ophemert**
Collection Date		01-12-2017	01-12-2017	01-12-2017	02-02-2018	02-02-2018	02-02-2018	20-03-2019	20-03-2019	21-03-2019
Mean Daily Q at Lobith (m^3/s)		3489	3489	3489	4740	4740	4740	5066	5066	4628
Water Level at Lobith (m +NAP)		11.05-11.55	11.05-11.55	11.05-11.55	12.40-12.90	12.40-12.90	12.40-12.90	12.40-12.90	12.40-12.90	12.40-12.90
ADCP Point Dataset Flow Velocity (m/s)	*min*	0.00	0.11	0.00	0.00	0.00	0.00	0.00	0.01	0.01
	max	1.99	1.77	2.25	3.39	2.44	3.39	2.14	2.28	2.64
3D Lattice Flow Velocity (m/s)	*min*	0.00	0.11	0.00	0.04	0.00	0.01	0.00	0.01	0.01
	max	1.99	1.77	2.25	2.6	2.31	3.34	2.14	2.26	2.6
Z-axis of 3D Lattice (m)	*min*	1.19	1.19	1.19	1.25	1.25	1.25	1.62	1.43	1.45
	max	6.69	6.69	7.19	8.25	8.25	8.25	8.12	8.93	8.45
Total Volume (m^3)		64,289	63,483	120,450	87,397	88,954	132,886	85,918	88,581	124,450

Passability Results												
Species	***Common name***	***Life Stage***										**Total Passess per Species**
**Anguilla anguilla (Linnaeus , 1758)*	European eel	J	52%?	-	-	49%**	-	-	43%?	24%?	-	**1**
Salmo trutta trutta (Linnaeus, 1758)	Sea trout	A	100%	100%	100%	100%	100%	97%	100%	100%	100%	**9**
Lampetra planeri (Bloch, 1784)	European brook lamprey	A	57%	93%**	87%**	55%	84%**	72%**	52%	31%	42%	**9**
**Chelon labrosus (Risso, 1827)*	Thicklip grey mullet	J	-	-	-	-	-	-	-	-	-	**0**
Gasterosteus aculeatus aculeatus (Linnaeus, 1758)	Three-spined stickleback	A	52%?	-	-	49%**	-	-	43%?	24%?	-	**1**
Alosa alosa (Linnaeus, 1758)	Allis shad	A	100%	100%	100%	98%	96%	97%	100%	100%	97%	**9**
Acipenser sturio (Linnaeus, 1758)	European sturgeon	A	100%	100%	100%	100%	100%	100%	100%	100%	100%	**9**
Alosa fallax fallax (Lacepède, 1803)	Twaite shad	A	98%	100%	97%	97%	96%	95%	98%	94%	96%	**9**
Coregonus lavaretus (Linnaeus, 1758)	European/common Whitefish	A	100%	100%	97%	98%	96%	97%	98%	95%	97%	**9**
Coregonus oxyrinchus (Linnaeus, 1758)	Houting	A	100%	100%	97%	98%	96%	97%	100%	95%	97%	**9**
Lampetra fluviatilis (Linnaeus, 1758)	River lamprey	A	92%	93%	87%	84%	84%	72%	95%	77%	83%	**9**
Osmerus eperlanus (Linnaeus, 1758)	European smelt	A	58%	95%**	90%**	56%	87%**	76%**	54%	33%	43%	**9**
Salmo salar (Linnaeus, 1758)	Atlantic salmon	A	100%	100%	100%	100%	100%	97%	100%	100%	100%	**9**
Petromyzon marinus (Linnaeus, 1758)	Sea lamprey	A	100%	100%	100%	98%	96%	97%	100%	100%	97%	**9**
Total Passes per Inflow			**11**	**11**	**11**	**13**	**11**	**11**	**11**	**11**	**11**	

Total counts excluded 'unlikely to pass' entries; "*" Catadromous species; "**" Passes using U_{burst}; "?" 'unlikely to pass' assigned; "-" 'does not pass' assigned; "J" denotes juveniles; "A" denotes adults.

distances ranged from 10 m for the thicklip grey mullet to 157 m for the European sturgeon.

3.2 Flow velocity 3D lattices

The flow velocity lattices (Tab. 1 and Fig. 3; see Fig. S1) had flow velocity minimum values that ranged from 0 to 0.11 m/s and maximum values ranging from 1.77 to 3.34 m/s (ADCP point datasets minimum range = 0–0.11 m/s and maximum range = 1.77–3.39 m/s. The Dreumel inflow 2017 lattice had the lowest maximum flow velocity value (1.77 m/s), meanwhile the highest was observed for the Ophemert inflow 2018 lattice (3.34 m/s). The Wamel inflow 2018 ADCP point data had a maximum flow velocity equal to 3.39 m/s, however this was only one data point with a high value. Voxler® calculated a maximum flow velocity for the Wamel inflow 2018 lattice equal to 2.60 m/s, corresponding with the second highest value of the ADCP point dataset.

The *z*-axis minimum value was observed for all of the inflow lattices in 2017 (1.19 m). The *z*-axis maximum value was observed for the Dreumel inflow 2019 lattice (8.93 m). The lattice volume minimum value was recorded for the Dreumel inflow 2017 lattice (63,483 m^3). The lattice volume maximum value was recorded for the Ophemert inflow 2018 lattice (132,886 m^3). The distance between lattice nodes ranged between 0.43–1.12, 0.32–1.40 and 0.03–0.04 m in the *x*, *y*, and *z*-axes, respectively.

3.3 LTD shore channel inflow passability by migratory fish

The final swimming speed lattices (Fig. 4) had ranges of negative and positive values denoting areas were the swimming speeds were lower or higher than the ambient flow velocities, respectively. The U_{crit} passability assessment for the high river discharge datasets resulted in a 'pass' being assigned for all lattices to the adults of each species with the

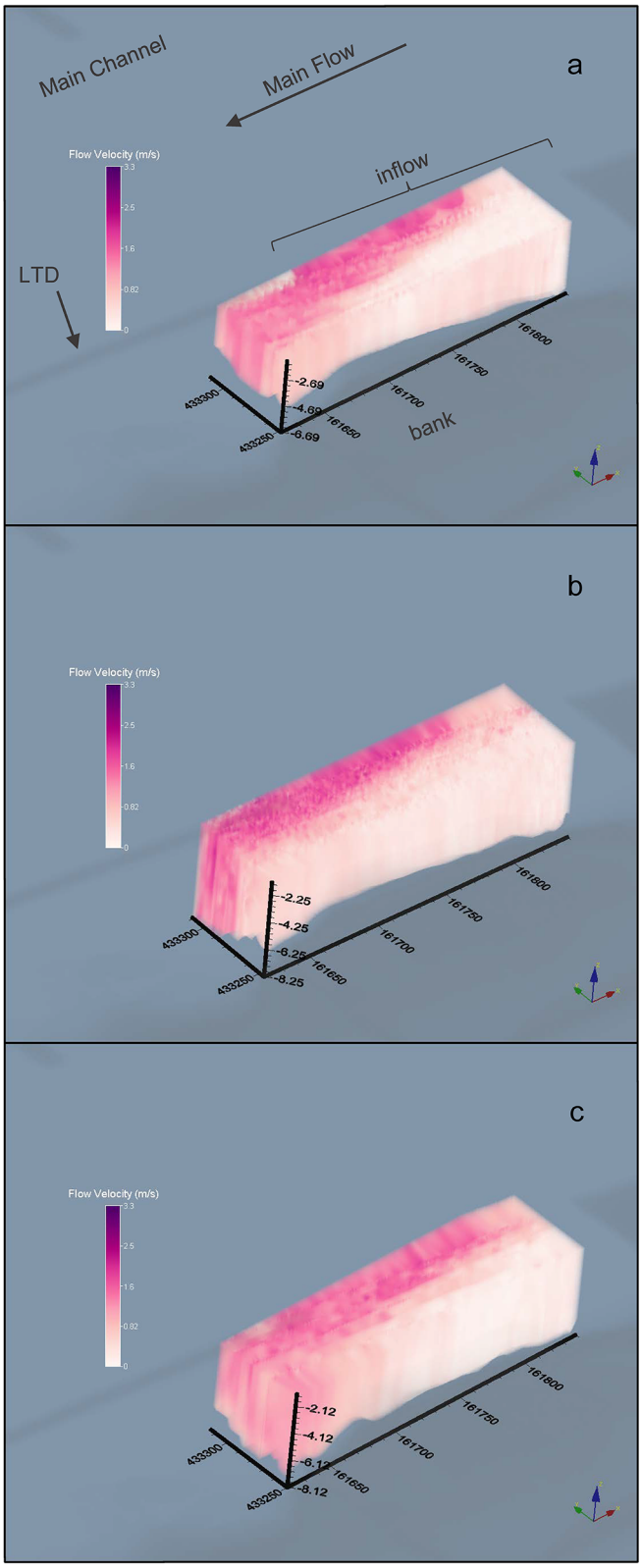

Fig. 3. The 3D lattices of the gridded flow velocities (m/s; 2 significant figures) for the Wamel shore channel inflow from ADCP data collected in (a) December 2017, (b) February 2018 and (c) March 2019. The *x*, *y* and *z* orientations are indicated by the arrows on the bottom-left corners.

exception of the three-spined stickleback, the European brook lamprey (*Lampetra planeri*; Bloch, 1784) and the European smelt (*Osmerus eperlanus*; Linnaeus, 1758). For those three species a 'pass' was occasionally assigned only after being assessed using U_{burst} (Tab. 1). Similarly, for the fish species assessed as juveniles, the European eel was only assigned one 'pass' while being assessed using U_{burst} and the thicklip grey mullet was assigned no passes.

Based on the number of fish species that passed each lattice, the inflows ranged from 79 to 93% passability. The Wamel inflow 2018 dataset had the highest passability, yet it was collected during relatively high river discharges ($Q = 4740\ m^3/s$). Calculated water column volume percentages for the passability of the fish species using U_{crit} ranged from 31 to 100%. Water column volume percentages for the passability of the fish species using U_{burst} ranged from 49 to 95%.

3.4 Statistical Analysis

The passability data consisted of count data for each inflow per year and hence was not normally distributed (p-value < 0.001). Based on the total number of passes, no significant association was found between the inflows and the year of data collection ($\chi^2 = 0.14658$, df = 4, p-value = 0.9974) this is likely due to the similar high river discharges of the datasets.

4 Discussion

4.1 Migratory fish species and passability indicators

The results obtained using the derived relationship between swimming speeds and fish length from Wolter and Arlinghaus (2003, 2004) were similar to those obtained in other swimming performance studies. The TL of the leptocephali stage of the European eel was used in our study, this was conservative as this is the size at which juveniles arrive at the European continental shelf from the spawning grounds in the Sargasso Sea (Kottelat and Freyhof, 2007). The yellow eel stage of the European eel has been observed during fish monitoring in the LTD shore channels (Collas *et al.*, 2020), hence it is likely that they reach this part of the river with larger TLs and hence could achieve higher U_{crit} and U_{burst}. Other studies have found U_{crit} equal to 0.43 m/s (0.04 m/s absolute difference; Quintella *et al.*, 2010) for yellow eels and U_{burst} equal to 7.5 BL (Body Lengths)/s (0.28 m/s absolute difference; McCleave, 1980) and 0.69 m/s (0.11 m/s absolute difference; Vowles *et al.*, 2015) for juvenile eels.

The European sturgeon had a TL (1250 mm) higher than that used to produce the swimming performance linear regressions in Wolter and Arlinghaus (2003; maximum TL = 1 m), which included data from other *Acipenser* species, such as *A. gueldenstaedtii*, and *A. stellatus*. The results for this species however are similar to those obtained in another study. U_{crit} studies on other *Acipenser* species have yielded results consistent with ours, such as 3.26 ± 0.11 BL/s (*Acipenser baeri*; 0.06–0.22 m/s absolute difference; Cai *et al.*, 2015) but also 1.63–2.4 TL/s (*Acipenser ruthenus*; 0.99–1.96 m/s absolute difference; Shivaramu *et al.*, 2019); however the

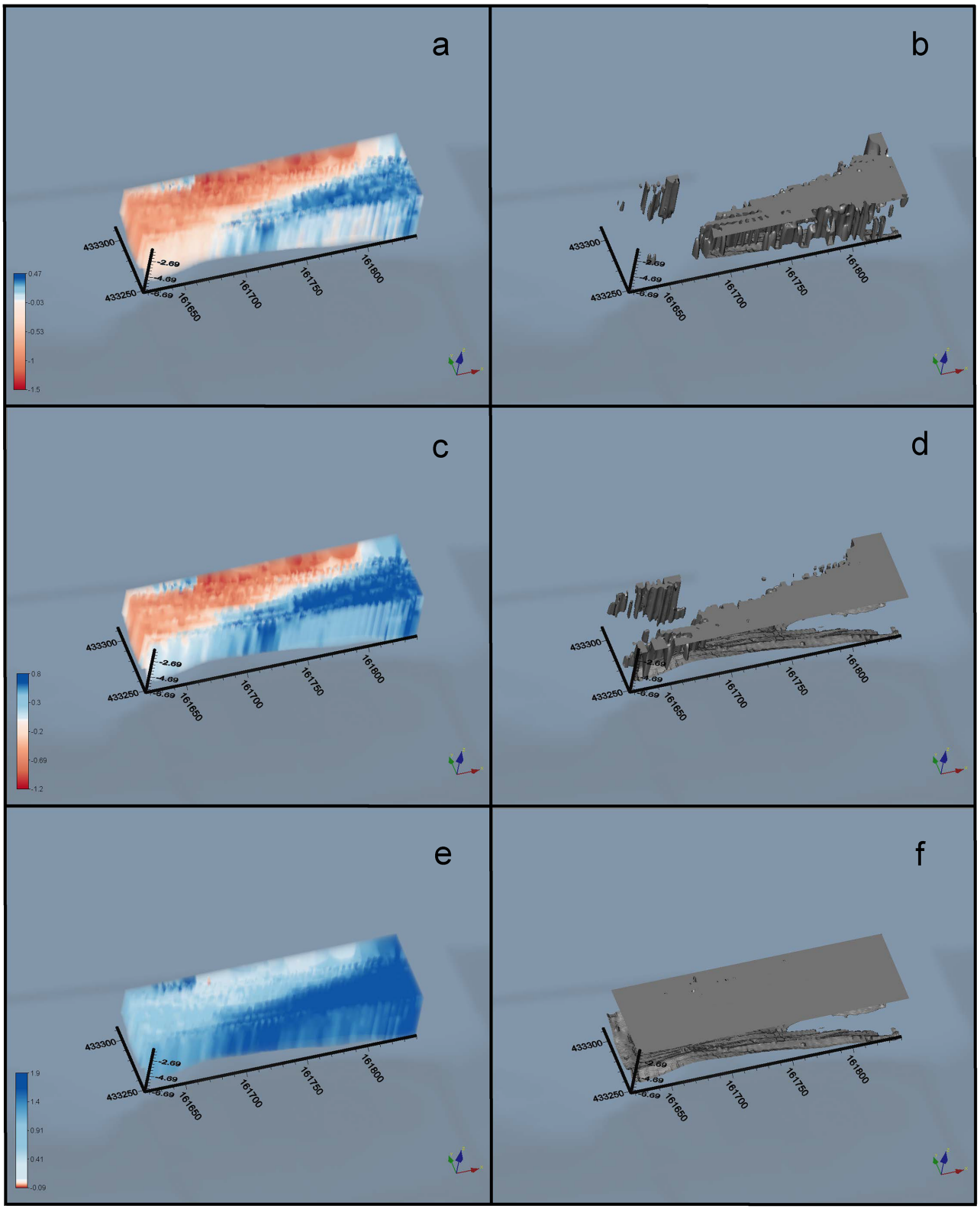

Fig. 4. Wamel inflow 2017 dataset final swimming speeds (m/s; 2 significant figures) for the European eel shown as (a) 3D lattice and (b) isosurface of passable lattice when using U_{crit}. The (c) 3D lattice and (d) isosurface of passable lattice when using U_{burst}. The (e) 3D lattice and (f) isosurface of passable lattice using U_{crit} for the twaite shad. All isosurfaces were estimated for final swimming speeds ≥0.05 m/s. Areas where some forward motion would be expected are shown in blue, neutral areas are shown in white and areas where the fish would be likely to drift are shown in red. The x, y and z orientations are indicated by the arrows on the bottom-left corners.

last study was performed on early life stages, which may explain the differing swimming performance.

Thicklip grey mullet has been found to have swimming speeds of 0.175 ± 0.041 m/s in laboratory experiments (0.03–0.12 m/s absolute difference with U_{crit}; Müller *et al.*, 1997). Schaarschmidt and Jürss (2003) reported mean U_{crit} for adult three-spined stickleback that ranged from 0.19 to 0.25 m/s (0.22–0.28 m/s absolute difference). While Taylor and McPhail (1985) found average speeds of 0.396 ± 0.0343 m/s (0.04-0.11 m/s absolute difference with U_{crit}). The U_{burst} in previous studies were equal to 0.661 ± 0.0430 m/s (0.10–0.18 m/s absolute difference; Taylor and McPhail, 1985) and as high as 1.314 ± 0.201 m/s (0.31–0.72 m/s absolute difference; Garenc *et al.*, 1999).

Some swimming performances from previous studies for species with high swimming speeds were comparable with our results. This included a U_{burst} range of 3.10–4.70 m/s for the Allis shad (Litaudon, 1985, as cited in Larinier and Travade, 2002). Further our result for the U_{burst} of Atlantic salmon falls within the range from a previous study by Colavecchia *et al.* (1998; 4.94–7.27 BL/s). Our approach has the limitation of applying the same regression equations to different fish species with different body shapes and fin forms, resulting in fish of the same TL but different species, body shapes and fin forms having the same passability results. However, this had the advantage of overcoming the differences in experimental design (*i.e.* swimming assessment time intervals, water temperature, *etc.*), as well as the over- or underrepresentation of some fish species in the scientific literature. Additionally, a recent study on the critical swimming performance of Iberian freshwater fish by Cano-Barbacil *et al.* (2020) that included different body shape, a calculated form factor, families and species, among five other parameters, concluded that body length was the most significant predictor for critical swimming performance. However the fish families and species were also found to play a significant role (Cano-Barbacil *et al.*, 2020). Hence the passability results may have been overestimated for fish species that specialize in slower swimming (*i.e.* anguilliform; Tytell *et al.*, 2010) and/or unsteady swimming (*i.e.* fast turns, change in direction, changes in speed, *etc.*), such as the European eel (Webb, 1984; Cano-Barbacil *et al.*, 2020).

4.2 Flow velocity 3D lattices

Innangi *et al.* (2016) used Voxler® in a similar approach in order to isolate parts of the water column using a dataset collected with a multibeam echosounder to identify fish schools, hence the software is suitable for this sort of 3D visualization of parameters in aquatic ecosystems. A limitation of our 3D lattice approach was that the densities of the ADCP data points differed per survey. This had an impact in the gridding process leading to differing distances between lattice nodes and localized flow velocity variations or clustering following the survey navigation tracklines. Another limitation is that the lattices are spatially restricted to the area covered by the ADCP point cloud in the x and y-axes. Hence the shallow areas, such as near the shore and the dams were not visualized. Yet some of these locations have some of the lowest flow velocities in the study sites leading to an underestimation of passability (Rhoads and Sukhodolov, 2001; Flores *et al.*, 2022). The z-axis of the lattices was also limited to the measurement heights of the ADCP datasets. This meant that the lattices did not reach the water surface and the riverbed at some areas, which are areas with high and low flow velocities, respectively (Carling, 1992; Rhoads and Sukhodolov, 2001). Our lattices do however spatially cover the navigable deepest sections of the water column available to migratory fish species. Some lattices also overlaid the dams, which is a likely occurrence since the dams become fully submerged during high discharges (water level $>$ 10 m + NAP at Lobith monitoring station; Normaal Amsterdams Peil, where 0 m + NAP is equal to the mean sea level of the North Sea). However, the exact submersion of the dams was not included in this study.

4.3 LTD shore channel inflow passability by migratory fish

Our assessment of the LTD shore channels inflow lattices showed that these study sites were not a bottleneck for 11 out of the 14 species assessed. The three fish species that had low passability concerned the juvenile stages of two catadromous species and the adult stage of the anadromous three-spined stickleback. The juvenile fish have the option of remaining in downstream river sections or inside the LTD shore channels if they enter through the outflows and/or during low river discharges until they have reached the length necessary to pass the inflows. Consequently, the small size of the three-spined stickleback adult makes it the most vulnerable of the fish species assessed, as it may be limited to remain downstream or within the LTD shore channels during comparable high river discharges. Since our results only represent several moments in time, the passability of the LTD inflows by small migratory fish species may not be completely impeded during the migration season. Instead there may be a migration delay during high river discharges. A delay could have other consequences such as shorter spawning periods if temperature requirements are not fully met in upstream spawning grounds, which can be worsened by climate change as average temperatures increase (LovellFord *et al.*, 2020; Xia *et al.*, 2021).

In a passability study conducted in France by Baudoin *et al.* (2015) that included several of the fish species in our study, the average and maximum swimming speeds used were higher than our estimated U_{crit} and U_{burst} speeds, hence our results were conservative. That study used a generalized approach that consisted of grouping similar fish species according to their swimming performance, hence our study based on TL is more size and life-stage specific. A limitation that may have led to overestimation of the passability for two fish species (sea trout, and three-spined stickleback) was the use of maximum lengths recorded for the Netherlands from www.beet.nl/records. Comparisons of passability based on the lower TL for adult males from www.fishbase.org (sea trout TL = 720 mm and three-spined stickleback TL = 51 mm) resulted in the same number of passes assigned to both species. It is important to note that our analysis considered small pockets of the water column (~1 m^3) as sufficient for recovery between swimming performances in the final swimming speeds lattices estimated using U_{crit}. This was seen as adequate since the weaker swimmers were very small (TL $<$ 160 mm).

Based on daily mean discharges of the river Rhine at the Lobith RWS monitoring station for the period after the construction of the LTDs (2015–2021; see Fig. S2; www.waterinfo.rws.nl), the mean discharge for the Rhine was estimated to be 2006 m^3/s. During the same time period, a total of 40–69 days in the winter months (December–February) had above mean river discharges. A total of 30–78 days in the spring months (March–May) had above mean river discharges. Lastly, a total of 0–86 days in the summer months (June–August) had above mean river discharges. The summer floods of 2016 (65 days) and 2021 (86 days) are good examples of the challenges that some migrating fish species may face in the river Waal during their upstream migration. The frequency and duration on these flooding events are expected to increase in the future due to climate change (Milly *et al.*, 2002; Van Vliet *et al.*, 2013). From the 14 fish species evaluated only 5 had migration periods outside of the months (December–March) when the ADCP datasets were collected (for species specific migration periods see Tab. S1). These species included the European brook lamprey, thicklip grey mullet, twaite shad, river lamprey and sea lamprey. These species had migration periods in the spring and summer months and thus they may also be impacted by flooding events during their migrations (April–July; see Fig. S2). Juvenile European eel have been observed in the North Sea during the winter months after which they start their upstream migration (Kottelat and Freyhof, 2007). Our results suggest that high discharges likely limited their passing of all of the study sites in 2017 and 2019. Nonetheless, the relationship between TL and swimming performance suggests that juvenile fish migrating upstream should be able to reach higher U_{crit} and U_{burst} as they grow larger, which may enable them to ultimately pass the inflows. The lowest TL assessed that was assigned a pass for all of the study sites in our study was equal to 160 mm. Further, the highest passability was seen at the Wamel shore channel inflow. Kasvi *et al.* (2017) described that in meandering rivers the highest velocities are present near the inner bank at the beginning of the river bend. The Wamel shore channel inflow is located near the beginning of the river bend, but a large part of the inflow area is protected by a wall, which may be reducing flow velocities in some areas near the inflow within the shore channel. Further the Ophemert inflow 2019 ADCP dataset was collected on a date were the daily mean river discharge had lowered to a value similar to that of the 2018 dataset, hence it is unclear how limiting this inflow was during the relatively higher discharges seen in 2019.

Fish monitoring of the LTD shore channels during the period 2016–2021 have yielded nine of the diadromous fish species in this study including the European eel, thicklip grey mullet, allis shad, houting, river lamprey, sea lamprey, Atlantic salmon, sea trout and three-spined stickleback (Collas et al., 2020, 2021; Flores and Collas, 2021). Additionally, a detection cable system (NEDAP) active in the Wamel and Ophemert shore channels since 2018 and outfitted to detect a few species of interest has detected tagged juvenile Atlantic salmon and adult European eel swimming downstream through the LTD shore channels (Collas *et al.*, 2020; Van de Ven, 2021a, 2021b). These records suggest that downstream migration through the study sites is possible for these diadromous fish species. Further diadromous fish species have been recorded swimming upstream possibly through the LTD shore channels. Adult sea trout specimens released downstream of the LTDs were detected swimming upstream through the LTD shore channels and one was later detected upstream of the LTDs in the German Rhine (Hop and Van de Ven, 2021). Likewise, several adult houting specimens released downstream have been detected in the winter entering and congregating in the Ophemert shore channel for possible spawning to then migrate back downstream. One houting was later detected in the German Rhine (Hop and Van de Ven, 2021). Further, a juvenile houting was caught in the Dreumel shore channel while fishing using a seine net during the summer of 2021 appearing to confirm the LTD shore channels as houting spawning grounds (Flores and Collas, 2021).

The inflows of the LTD shore channels have sills that are often modified for water management purposes. In 2017 the sill of the Wamel inflow was open, then it was closed in April of 2018. The Dreumel inflow sill was raised in April 2018 remaining unchanged during the collection of the 2019 ADCP dataset (Personal communication with H. Eerden; project manager of RWS; 21 March 2022). Unexpectedly, the higher passability in the Wamel inflow in 2018 appears related to the higher daily mean river discharge during the collection of that ADCP dataset, this since the changes to the sill occurred later that year. These higher passability results may be due to the geometry of the Wamel inflow area, possibly in combination with changes in riverbed elevation that occur in a meandering river during a flood (*i.e.* deposition and erosion in the littoral zone; Kasvi *et al.*, 2017). It is possible that river discharges like those that occurred during the collection of the 2018 dataset, might reach areas in the sloping banks that result in shallow areas with lower flow velocity ranges at that study site. Meanwhile, floods with relatively low river discharges do not reach those same banks or do not result in water levels high enough to survey with an ADCP. On the other hand, floods with relatively high river discharges like those that occurred during the collection of the 2019 dataset, may result in flow velocity ranges in those same banks that are considered moderate to high for upstream migrating fish. Also, the lower passability in Wamel in 2019 could be partially due to the changes to the sill, but this is unlikely since the results are equal to those seen in 2017 before the changes were made. The changes to the Dreumel inflow seem to not have affected passability for the 2019 dataset, which was collected after the alterations to that sill. After the sill modifications, large fish should still be able to migrate through during months with high river discharges as the sills were fully submerged. A possible management option could be to maximize the cross-sectional area of the sills, which could lower the flow velocities during high river discharges thus aiding the upstream migration of smaller fish. We also recommend encouraging the development of gradually sloping shorelines, since these shallower littoral zones tend to have lower flow velocities.

Future passability analyses could focus more on species of interest by using swimming performances available from the scientific literature. Later assessments should aim at including the submersion of the dams, evaluating a larger area of the water column and using or collecting ADCP datasets with higher spatial coverage. This could be achieved by using an ACDP drone system which are able to survey in shallower areas. Continuously collected ADCP datasets could also be beneficial to constantly assess passability through time. This may

help to elucidate what different sill geometries and/or river discharges mean for the passability of migratory fish. An assessment of surrounding groyne fields and other areas of the main channel should also be completed for comparison purposes. Lastly, the flow velocity monitoring datasets used in this assessment represent several single moments in time that may not characterize the flow conditions for the entire migration period of the fish species. Hence we recommend that in future research this assessment should be repeated for at least every river discharge change event during the entire migration period of the fish species of interest. Future assessments should also include data from upstream migrating individuals of various lengths. Data on the migration of telemetrically tracked fish species migrating upstream in the Waal, such as the houting or the sea trout, could be used to validate the results of passability assessments.

5 Conclusions

Our approach offers the advantage of using monitoring data to assess ambient flow velocities in the water column resulting from river training structures in 3D and their passability for many fish species and at different life stages. Juveniles with a TL equal to or larger than 70 mm were predicted to pass the Wamel inflow during the flood of 2018 while using U_{burst}. All adult stages assessed were able to pass the three inflows with the exception of *Gasterosteus aculeatus aculeatus*, which was predicted to not pass most high discharge conditions due to its small size. The minimum fish TL assessed that was assigned a pass for all of the LTD inflows during the high river discharges was equal to 160 mm. Among all of the study sites, the Wamel inflow on the 2nd of February in 2018 showed the highest passability. A management option for the inflow sills could be to increase the cross-sectional area in order to facilitate fish migration through the reduction of flow velocities during high river discharges. Additionally the development of gradually sloping shorelines should be encouraged since those shallower areas tend to have lower flow velocities.

Data sharing

The data are archived in the Dans Easy repository of the Radboud University (https://doi.org/10.17026/dans-xtm-cyhg).

Supplementary Material

Table S1. Migratory fish species included in the passability assessment of the LTD shore channels inflows.
Table S2. Final swimming velocity threshold test for different significance levels done for all of the yearly datasets for *Anguilla anguilla*.
Figure S1. The 3D lattices of the gridded flow velocities (m/s; 2 significant figures) for the Dreumel shore channel inflow from ADCP data collected in (a) December 2017, (b) February 2018, and (c) March 2019. The gridded flow velocities for the Ophemert shore channel inflow from ADCP data collected in (d) December 2017, (e) February 2018, and (f) March 2019. The x, y and z orientations are indicated by the arrows on the bottom-left corners.
Figure S2. Hydrograph for the river Rhine at the Lobith RWS monitoring station from 2015-2021 (www.waterinfo.rws.nl). Superimposed are the migration periods for the five fish species with migrations outside of the ADCP data collection dates. The dashed grey lines denote the minimum and maximum river discharges during which ADCP data was collected. The graph shows that high river discharges ($\geq$ 3489 m^3 /s) have also occurred during those periods since the construction of the LTDs.

The Supplementary Material is available at https://www.kmae.org/10.1051/kmae/2022019/olm.

Acknowledgments. Rijkswaterstaat (RWS) Oost Nederland funded this study (Reference RWS 31153573). We are very thankful to Bert Go (RWS) for his help in procuring the datasets and to Margriet Schoor (RWS) and Henk Eerden (RWS) for their advice and support during the completion of this study.

References

Aarts BG, Nienhuis PH. 2003. Fish zonations and guilds as the basis for assessment of ecological integrity of large rivers. *Hydrobiologia* 500: 157–178.
Baudoin JM, Burgun V, Matthieu C, *et al.* 2015. Assessing the passage of obstacles by fish. Concepts, design and application. The National Agency for Water and Aquatic Environments (Onema), Vincennes, France, 54 pp.
Beamish FWH, 1978. Swimming capacity. In Hoar WS & Ran-dall DJ, eds. Fish physiology. New York, NY: Academic Press, pp. 101–187.
Binohlan C, Froese R, Pauly D, Reyes R. 2011. The length-length table in FishBase. In Froese R & Pauly D, eds. FishBase. World Wide Web electronic publication. www.fishbase.org. Accessed 10 October 2020.
Brett J. 1964. The respiratory metabolism and swimming performance of young sockeye salmon. *J Fish Res Board Can* 21: 1183–1226.
Buchanan TJ, Somers WP. 1969. Discharge measurements at gaging stations. Report 03-A8. United States Government Printing Office, Washington D.C., the United States, pp. 1.
Cai L, Johnson D, Mandal P, *et al.* 2015. Effect of exhaustive exercise on the swimming capability and metabolism of juvenile Siberian sturgeon. *Trans Am Fish Soc* 144: 532–538.
Cano-Barbacil C, Radinger J, Argudo M, Rubio-Gracia F, Vila-Gispert A, García-Berthou E. 2020. Key factors explaining critical swimming speed in freshwater fish: a review and statistical analysis for Iberian species. *Sci Rep* 10.
Carling PA. 1992. The nature of the fluid boundary layer and the selection of parameters for benthic ecology. *Freshw Biol* 28: 273–284.
Colavecchia M, Katopodis C, Goosney R, Scruton DA, McKinley RS. 1998. Measurement of burst swimming performance in wild Atlantic salmon (*Salmo salar* L.) using digital telemetry. *Regul Rivers: Res Mgmt* 14: 41–51.
Collas FPL, Buijse AD, Van den Heuvel F L, *et al.* 2018. Longitudinal training dams mitigate effects of shipping on environmental conditions and fish density in the littoral zones of the river Rhine. *Sci Total Environ* 619–620: 1183–1193.
Collas FPL, Flores NY, Van Aalderen R, *et al.* 2020. Rapportage natuurgegevens langsdammen Waal 2016–2020. Series of Reports on Animal Ecology and Physiology 2020-2, Radboud University, Nijmegen, the Netherlands, pp. 56–60 (in Dutch).

Collas FPL, Van Aalderen R, Scharbert AP, Leuven RSEW. 2021. Stow net fishing in the river Rhine 2018–2021. Series of Reports on Animal Ecology and Physiology 2021-3, Radboud University, Nijmegen, the Netherlands, pp. 3–20.

Deinet S, Scott-Gatty K, Rotton H, *et al.* 2020. The Living Planet Index (LPI) for migratory freshwater fish – Technical Report. World Fish Migration Foundation, Groningen, the Netherlands, pp. 6.

Del Signore A, Lenders HJR, Hendriks AJ, Vonk JA, Mulder C, Leuven RSEW. 2016. Size-mediated effects of water-flow velocity on riverine fish species. *River Res Appl* 32: 390–398.

De Ruijsscher TV, Naqshband S, Hoitink T. 2018. Flow bifurcation at a longitudinal training dam: effects on local morphology. *E3S Web Conf* 40: 05020.

De Ruijsscher TV, Vermeulen B, Hoitink AJF. 2020. Diversion of flow and sediment towards a side channel separated from a river by a longitudinal training dam. *Water Resour Res* 56: e2019WR026750.

Eerden H. 2013. Pilot langsdammen Waal: projectplan realisatiefase II monitoren & inregelen – projectfase MIRT4. Concept Projectplan versie 1.0. Bijlage D: Monitoringsplan Pilot Langsdammen Waal. Ministerie van Infrastructuur en Milieu, Rijkswaterstaat Oost Nederland, Arnhem, the Netherlands (in Dutch).

Flores NY, Collas FPL. 2021. Mitigation of inland navigation effects on biodiversity by longitudinal training dams. Series of Reports on Animal Ecology and Physiology 2021-9. Radboud University, Nijmegen, the Netherlands, pp. 36–38.

Flores NY, Collas FPL, Mehler K, Schoor MM, Feld CK, Leuven RSEW. 2022. Assessing habitat suitability for native and alien freshwater mussels in the river Waal (the Netherlands), using hydroacoustics and species sensitivity distributions. *Environ Model Assess* 27: 187–204.

Garenc C, Couture P, Laflamme MA, Guderley H. 1999. Metabolic correlates of burst swimming capacity of juvenile and adult threespine stickleback (*Gasterosteus aculeatus*). *J Comp Physiol B* 169: 113–122.

Grill G, Lehner B, Thieme M, *et al.* 2019. Mapping the world's free-flowing rivers. *Nature* 569: 215–221.

Hop J, Van de Ven M. 2021. Migration of adult diadromous fish in the Rhine delta: analysis of NEDAP traildata 2017–2020. Report number 20191133/03, ATKB, Rotterdam, the Netherlands, pp. 15–50.

Innangi S, Bonanno A, Tonielli R, François G, Innangi M, Sandro M. 2016. High resolution 3-D shapes of fish schools: A new method to use the water column backscatter from hydrographic multibeam echo sounders. *Appl Acoust* 111: 148–160.

Kasvi E, Laamanen L, Lotsari E, Alho P. 2017. Flow patterns and morphological changes in a sandy meander bend during a flood—spatially and temporally intensive ADCP measurement approach. *Water* 9: 106.

Katopodis C. 1992. Introduction to fishway design. Freshwater Institute, Department of Fisheries and Oceans Canada, Winnipeg, Manitoba, Canada, 35 pp.

Kottelat M, Freyhof J. 2007. Handbook of European freshwater fishes. Publications Kollelat, Cornol, and Freyhof, Berlin, 61–465 pp.

Kucera-Hirzinger V, Schludermann E, Zornig H, Weissenbachter A, Schabuss M, Schiemer F. 2009. Potential effects of navigation-induced wave wash on the early life history stages of riverine fish. *Aquat Sci* 71: 94–102.

Larinier M, Travade F. 2002. Designing fish passage facilities for shad. *Bull Fr Pêche Piscic* 364: 135–146.

Limburg KE, Waldman JR. 2009. Dramatic declines in north Atlantic diadromous fishes. *BioScience* 59: 955–965.

Litaudon A. 1985. Preliminary observations on shad (*Alosa alosa*) passing the Saint-Laurent-des-Eaux (Loire) weir. Report HE/31/85-37. Électricité de France, Paris, France, pp. 63 (in French).

LovellFord RM, Flitcroft RL, Lewis SL, Santelmann MV, Grant GE. 2020. Patterns of river discharge and temperature differentially influence migration and spawn timing for Coho salmon in the Umpqua River Basin, Oregon. *Trans Am Fish Soc* 149: 695–708.

McCleave JD. 1980. Swimming performance of European eel (*Anguilla anguilla* L.) elvers. *J Fish Biol* 16: 445–452.

Milly P, Wetherald R, Dunne K, Delworth TL. 2002. Increasing risk of great floods in a changing climate. *Nature* 415: 514–517.

Müller UK, Van den Heuvel BLE, Stamhuis EJ, Videler J. 1997. Fish foot prints: morphology and energetics of the wake behind a continuously swimming mullet (*Chelon labrosus* Risso). *J Exp Biol* 200: 2893–2906.

Myers GS. 1949. Usage of anadromous, catadromous and allied terms for migratory fishes. *Copeia* 1949: 89–97.

Quintella B, Mateus C, Costa J, Domingos I, Almeida P. 2010. Critical swimming speed of yellow- and silver-phase European eel (*Anguilla anguilla*, L.). *J Appl Ichthyol* 26: 432–435.

R Core Team. 2021. R: A language and environment for statistical computing. R Foundation for Statistical Computing, Vienna, Austria. URL https://www.R-project.org/. Accessed 20 April 2021.

Raat AJP. 2001. Ecological rehabilitation of the Dutch part of the River Rhine with special attention to the fish. *Regul River* 17: 131–144.

Rand PS, Hinch SG, Morrison J, *et al.* 2006. Effects of river discharge, temperature, and future climates on energetics and mortality of adult migrating Fraser river sockeye salmon. *Trans Am Fish Soc* 135: 655–667.

Rhoads B, Sukhodolov A. 2001. Field investigation of three-dimensional flow structure at stream confluences: 1. Thermal mixing and time-averaged velocities. *Water Resour Res* 37 2393–2410.

Schaarschmidt T, Jürss K. 2003. Locomotory capacity of Baltic Sea and freshwater populations of the threespine stickleback (*Gasterosteus aculeatus*). *Comp Biochem Phys A* 135: 411–424.

Shivaramu S, Santo CE, Kašpar V, *et al.* 2019. Critical swimming speed of sterlet (*Acipenser ruthenus*): Does intraspecific hybridization affect swimming performance? *J Appl Ichthyol* 35: 217–225.

Taylor E, McPhail J. 1985. Prolonged and burst swimming in anadromous and freshwater threespine stickleback, *Gasterosteus aculeatus*. *Can J Zool* 64: 416–420.

Tytell E, Borazjani I, Sotiropoulos F, Baker T, Anderson E, Lauder G. 2010. Disentangling the functional roles of morphology and motion in the swimming of fish. *Integr Comp Biol* 50: 1140–1154.

Uehlinger U, Wantzen K, Leuven RSEW, Arndt H. 2009. The Rhine River Basin. In Tockner K, Uehlinger U, Robinson CT, eds. Rivers of Europe. London: Academic Press, pp. 199–245.

Van de Ven M. 2021a. Telemetric study on the migration of female silver eels in the river Rhine cohorts 2018 and 2019. Report number 20191133/01, PKB, Rotterdam, the Netherlands, pp. 32–46.

Van de Ven M. 2021b. Telemetric study on the migration of salmon smolts in the river Rhine cohorts 2018 and 2020. Report number 20191133/02, PKB, Rotterdam, the Netherlands, pp. 15–46.

Van Vliet MTH, Ludwig F, Kabat P. 2013. Global streamflow and thermal habitats of freshwater fishes under climate change. *Clim Change* 121: 739–754.

Vowles AS, Don AM, Karageorgopoulos P, Worthington TA, Kemp PS. 2015. Efficiency of a dual density studded fish pass designed to mitigate

for impeded upstream passage of juvenile European eels (*Anguilla anguilla*) at a model Crump weir. *Fish Manag Ecol* 22: 307–316.

Webb PW. 1984. Body form, locomotion and foraging in aquatic vertebrates. *Am Zool* 24: 107–120.

Westenbroek SM. 2006. Estimates of shear stress and measurements of water levels in the lower Fox River near Green Bay, Wisconsin. Scientific Investigations Report 2006–5226. U. S. Geological Survey, Reston, the United States, pp. 5–29.

Wolter C, Arlinghaus R. 2003. Navigation impacts on freshwater fish assemblages: the ecological relevance of swimming performance. *Rev Fish Biol Fisher* 13: 63–89.

Wolter C, Arlinghaus R. 2004. Burst and critical swimming speed of fish and their ecological relevance in waterways. Report 20/2004. Leibniz-Institut für Gewässerökologie und Binnenfischerei (IGB), Berlin, Germany, pp. 77–93.

Xia Y, Li X, Yang J, *et al.* 2021. Elevated temperatures shorten the spawning period of silver carp (*Hypophthalmichthys molitrix*) in a large subtropical river in China. *Front Mar Sci* 8: 708109.

Zajicek P, Johannes R, Wolter C. 2018. Disentangling multiple pressures on fish assemblages in large rivers. *Sci Total Environ* 627: 1093–1105.

Cite this article as: Flores NY, Collas FPL, Leuven RSEW. 2022. 3D upstream passability of novel river training structures by migratory fish in the river Waal. *Knowl. Manag. Aquat. Ecosyst.*, 423, 23.